

Circulation

JOURNAL OF THE AMERICAN HEART ASSOCIATION



Evidence for Microvascular Dysfunction in Hypertrophic Cardiomyopathy: New Insights From Multiparametric Magnetic Resonance Imaging

Steffen E. Petersen, Michael Jerosch-Herold, Lucy E. Hudsmith, Matthew D. Robson, Jane M. Francis, Helen A. Doll, Joseph B. Selvanayagam, Stefan Neubauer and Hugh Watkins

Circulation 2007;115:2418-2425; originally published online Apr 23, 2007;

DOI: 10.1161/CIRCULATIONAHA.106.657023

Circulation is published by the American Heart Association, 7272 Greenville Avenue, Dallas, TX 75214

Copyright © 2007 American Heart Association. All rights reserved. Print ISSN: 0009-7322. Online ISSN: 1524-4539

The online version of this article, along with updated information and services, is located on the World Wide Web at:

<http://circ.ahajournals.org/cgi/content/full/115/18/2418>

Data Supplement (unedited) at:

<http://circ.ahajournals.org/cgi/content/full/CIRCULATIONAHA.106.657023/DC1>

Subscriptions: Information about subscribing to *Circulation* is online at
<http://circ.ahajournals.org/subscriptions/>

Permissions: Permissions & Rights Desk, Lippincott Williams & Wilkins, a division of Wolters Kluwer Health, 351 West Camden Street, Baltimore, MD 21202-2436. Phone: 410-528-4050. Fax: 410-528-8550. E-mail:
journalpermissions@lww.com

Reprints: Information about reprints can be found online at
<http://www.lww.com/reprints>

Evidence for Microvascular Dysfunction in Hypertrophic Cardiomyopathy

New Insights From Multiparametric Magnetic Resonance Imaging

Steffen E. Petersen, MD, DPhil; Michael Jerosch-Herold, PhD; Lucy E. Hudsmith, MA, MRCP; Matthew D. Robson, MA, PhD; Jane M. Francis, DCR, DNM; Helen A. Doll, MSc, DPhil; Joseph B. Selvanayagam, MBBS, FRACP, DPhil; Stefan Neubauer, MD, FRCP; Hugh Watkins, MD, PhD, FRCP

Background—Microvascular dysfunction in hypertrophic cardiomyopathy (HCM) may create an ischemic substrate conducive to sudden death, but it remains unknown whether the extent of hypertrophy is associated with proportionally poorer perfusion reserve. Comparisons between magnitude of hypertrophy, impairment of perfusion reserve, and extent of fibrosis may offer new insights for future clinical risk stratification in HCM but require multiparametric imaging with high spatial and temporal resolution.

Methods and Results—Degree of hypertrophy, myocardial blood flow at rest and during hyperemia (hMBF), and myocardial fibrosis were assessed with magnetic resonance imaging in 35 HCM patients (9 [26%] male/26 female) and 14 healthy controls (4 [29%] male/10 female), aged 18 to 78 years (mean±SD, 42±14 years) with the use of the American Heart Association left ventricular 16-segment model. Resting MBF was similar in HCM patients and controls. hMBF was lower in HCM patients (1.84±0.89 mL/min per gram) than in healthy controls (3.42±1.76 mL/min per gram, with a difference of -0.95 ± 0.30 [SE] mL/min per gram; $P<0.001$) after adjustment for multiple variables, including end-diastolic segmental wall thickness ($P<0.001$). In HCM patients, hMBF decreased with increasing end-diastolic wall thickness ($P<0.005$) and preferentially in the endocardial layer. The frequency of endocardial hMBF falling below epicardial hMBF rose with wall thickness ($P=0.045$), as did the incidence of fibrosis ($P<0.001$).

Conclusions—In HCM the vasodilator response is reduced, particularly in the endocardium, and in proportion to the magnitude of hypertrophy. Microvascular dysfunction and subsequent ischemia may be important components of the risk attributable to HCM. (*Circulation*. 2007;115:2418-2425.)

Key Words: cardiomyopathy ■ contrast media ■ fibrosis ■ magnetic resonance imaging ■ perfusion

Hypertrophic cardiomyopathy (HCM) is a disease entity characterized by the development of cardiac hypertrophy without an obvious extrinsic cause, such as pressure or volume overload, and is a disease of the sarcomere.¹ Sudden cardiac death is a well-recognized feature of this disease, and HCM is the most common cause of sudden death in the younger population, particularly in young athletes.² The risk of sudden cardiac death increases with multiple clinical risk factors, such as nonsustained ventricular tachycardia, syncope, exercise blood pressure response, family history of sudden death, and extreme left ventricular (LV) hypertrophy.³ In addition, marked LV outflow tract obstruction and coronary microvascular dysfunction have been found to be independent predictors of sudden death in HCM.^{4,5} Moon and colleagues⁶ demonstrated an association between the extent

Clinical Perspective p 2425

of myocardial fibrosis and progressive ventricular dilatation and markers of sudden death.

Although adverse microvascular remodeling and coronary microvascular dysfunction, reflected by an inadequate increase in myocardial blood flow (MBF) in response to a coronary vasodilator, has been noted in HCM, it remains unknown whether the impairment of the hyperemic response is related to the degree of LV hypertrophy.^{5,7-12} Hypertrophy is an independent risk factor for sudden death in HCM, but the underlying mechanism is unclear; potentially sudden death could be associated with impaired myocardial perfusion or extent of myocardial fibrosis. Current risk factor stratification does not assess either of these parameters reliably.³

Received August 7, 2006; accepted March 2, 2007.

From the Department of Cardiovascular Medicine and University of Oxford Centre for Clinical Magnetic Resonance Research, University of Oxford, Oxford, UK (S.E.P., L.E.H., M.D.R., J.M.F., J.B.S., S.N., H.W.); Advanced Imaging Research Center, Oregon Health & Science University, Portland, Ore (M.J.-H.); and Department of Public Health, University of Oxford, Oxford, UK (H.A.D.).

The online-only Data Supplement, consisting of an addendum with figures, is available with this article at <http://circ.ahajournals.org/cgi/content/full/CIRCULATIONAHA.106.657023/DC1>.

Correspondence to Steffen E. Petersen, MD, DPhil, University of Oxford Centre for Clinical Magnetic Resonance Research, Department of Cardiovascular Medicine, John Radcliffe Hospital, Oxford, OX3 9DU, UK. E-mail steffen.petersen@cardiov.ox.ac.uk

© 2007 American Heart Association, Inc.

Circulation is available at <http://www.circulationaha.org>

DOI: 10.1161/CIRCULATIONAHA.106.657023

Cardiovascular magnetic resonance imaging (MRI) during the first pass of a contrast agent allows the evaluation of myocardial perfusion both at rest and during pharmacological stress. Cardiovascular MRI first-pass perfusion is an attractive novel methodology with which to explore the uncertainties regarding myocardial perfusion in HCM: First, it has been validated against the gold standard of microspheres¹³; second, it is characterized by superior spatial resolution compared with nuclear imaging methods (including positron emission tomography [PET]), permitting the assessment of transmural perfusion gradients; third, myocardial perfusion can be quantified in absolute terms in milliliters per minute per gram, which has the advantage of identifying abnormalities in perfusion that lead to spatially coherent reductions in both rest and stress perfusion, therefore potentially creating the misleading impression of a “normal” perfusion reserve; fourth, cardiovascular MRI first-pass perfusion data can be matched within given myocardial segments to other important parameters provided by cardiovascular MRI for risk stratification, such as wall thickness or extent of fibrosis, which cannot be provided by any other single imaging modality.¹⁴

In the present study we assessed the association of blood flow in relation to wall thickness and extent of fibrosis with the use of high-resolution quantitative cardiovascular MRI. Advancing knowledge and understanding of these pathophysiological interrelations may form an important initial step toward improved clinical risk assessment for sudden cardiac death in HCM.

Methods

Ethics and Study Population

The study was approved by our institutional ethics committee, and informed written consent was obtained from each patient. All MRI data were analyzed in a blinded manner.

Thirty-five consecutive patients with HCM from the University of Oxford Cardiomyopathy Clinic (9 male/26 female; mean age, 44 ± 15 years) and 14 healthy controls (4 male/10 female; mean age, 39 ± 11 years) were enrolled into the study. The diagnosis of HCM was based on genetic confirmation of a pathogenic mutation, or when no genetic confirmation of HCM was available, it was based on the conventional criteria of LV hypertrophy not originating from other causes (≥ 15 mm or ≥ 13 mm in documented familial disease) determined by echocardiography.¹⁵ Healthy volunteers had no history of cardiac disease, hypertension, and other cardiac risk factors and had a normal 12-lead ECG.

Subjects with contraindications for MRI were not enrolled. Typical contraindications for adenosine applied, including asthma and higher degree of heart block. All subjects undergoing adenosine administration had abstained from caffeine intake for at least 12 hours before the study. Table 1 highlights characteristics of HCM patients and healthy subjects.

MRI Protocol

All cardiovascular MRI examinations were performed on a 1.5-T MRI system (Sonata; Siemens Medical Solutions, Erlangen, Germany). After scout imaging was performed, steady state free precession cine images were acquired in horizontal and vertical long-axis views, and short-axis views were obtained parallel to the atrioventricular groove and included the entire LV.¹⁶

A gadolinium-based contrast agent (gadodiamide [Omniscan]; Nycomed Amersham, Amersham, UK) was then administered intravenously as a bolus at a dose of 0.025 mmol/kg body wt (injection rate, 5 mL/s; concentration, 0.5 mmol/mL), followed by a saline

TABLE 1. Baseline Characteristics of Healthy Controls and HCM Patients

	HCM Patients (n=35)	Healthy Controls (n=14)	P
Age, y	44±15	39±11	0.304
Male gender, %	26	29	0.878
Diabetes	0	0	...
Current smoking, n (%)	1 (3)	0	0.651
Weight, kg	80.3±16.0	79.3±9.9	0.788
Height, cm	174.2±10.9	179.4±9.9	0.116
Body surface area, m ²	1.96±0.24	1.98±0.17	0.801
Heart rate, bpm	57±8	60±12	0.426
Mean arterial pressure, mm Hg	92±8	97±11	0.168
LV EDV index, mL/m ²	78±15	77±15	0.867
LV ESV index, mL/m ²	21±12	22±5	0.658
LV ejection fraction, %	74±9	71±4	0.194
Maximum end-diastolic wall thickness, mm	16.7±6.1	10.2±1.4	<0.0001*
LV mass index, g/m ²	88.1±31.2	64.9±13.3	0.0006*

Values are mean±SD unless otherwise indicated. EDV indicates end-diastolic volume; ESV, end-systolic volume.

*Statistical significance at $P<0.05$.

flush of 13 mL at the same rate. Perfusion imaging was performed every heartbeat during the first pass of the contrast bolus with the use of a T1-weighted fast (spoiled) gradient echo sequence with saturation-recovery magnetization preparation, as described previously.¹⁴ Perfusion images were acquired in 3 short-axis sections at basal (between LV outflow tract and the papillary muscles), midventricular, and apical levels chosen according to recommended guidelines.¹⁷ To allow sufficient contrast washout, we performed stress perfusion imaging 10 minutes after the study at rest. Adenosine was used as the pharmacological vasodilator and was administered at a rate of 140 $\mu\text{g}/\text{kg}$ per minute for at least 2 minutes before and during data acquisition. After stress perfusion imaging, we gave an additional dose of 0.1 mmol/kg gadodiamide to reach a total administered dose of 0.15 mmol/kg. The delayed enhancement images were acquired after an additional 10-minute delay with the use of an inversion-recovery prepared, segmented gradient echo sequence, as previously described (Figure 1).^{18,19}

Image Analysis

Both global LV function and segmental wall thickness were analyzed with the use of commercially available computer software by manual tracing of endocardial and epicardial contours (Argus and Syngo2002B; Siemens Medical Solutions, Erlangen, Germany). The following global parameters (normalized to the body surface area) were determined by planimetry of short-axis cine images: LV end-diastolic volume index (mL/m²), LV end-systolic volume index (mL/m²), LV stroke volume index (mL/m²), LV ejection fraction (%), and LV mass index (g/m²). End-diastolic wall thickness was determined in 6 basal, 6 midventricular, and 4 apical segments.¹⁷

For perfusion analysis, the endocardial and epicardial contours were traced manually with the use of the software MRI-MASS (Medis, Leiden, the Netherlands). Again, the myocardium was divided into 16 corresponding segments and was further subdivided into endocardial (inner 50% of transmural thickness) and epicardial (outer 50% of transmural thickness) layers. MBF was determined by model-independent deconvolution of signal intensity curves with an arterial input function measured in the LV blood pool,¹³ with explicit accounting for any delay in the arrival of the tracer (Figure 2).²⁰ Details about the estimation of MBF are provided in the online-only Data Supplement.

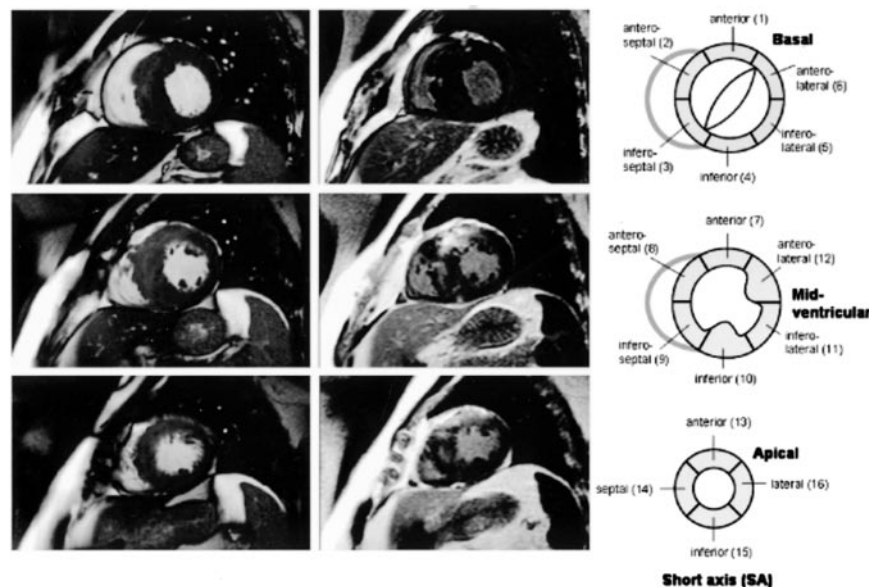


Figure 1. MRI of 31-year-old male patient with HCM demonstrating asymmetrical LV hypertrophy and fibrosis in basal (top row), midventricular (middle row), and apical (bottom row) short-axis slices. The schematic represents the segmentation used as recommended by the American Heart Association and the American College of Cardiology.¹⁷

Delayed contrast-enhanced images were quantified with the use of computer-assisted planimetry with a 16-segment model identical to that described above. Hyperenhanced pixels were defined as those with signal intensities >2 SD above the mean signal intensity in remote myocardium in the same slice.²¹ The segmental extent of fibrosis was expressed as a percentage of hyperenhanced pixels within each segment [ie, segmental extent of fibrosis = $100 \times$ hyperenhanced pixels / (hyperenhanced + nonhyperenhanced pixels)]. The incidence of fibrosis was a dichotomous parameter based on presence or absence of hyperenhancement within each segment.

Statistical Analysis

Values are expressed as mean \pm SD. Regression analysis with the use of linear mixed-effects models with a random intercept for subject was performed to take account of within-patient correlations of repeated measurements.²² The analysis was performed in the R

statistical analysis environment (R, version 2.3.1; The R Foundation for Statistical Computing, Vienna, Austria, 2006; <http://www.r-project.org/>). Linear regression models were used to test for significant associations between resting or hyperemic blood flow and end-diastolic wall thickness as a measure of the magnitude of hypertrophy. The dependent variable was adjusted in the fixed-effects part of the linear mixed-effects model for differences in age, gender, rate-pressure product at rest (in the case of resting MBF), extent of contrast enhancement, and HCM diagnosis. For hyperemic MBF (hMBF) as the dependent variable, we additionally tested for the hypothesis that the presence of LV outflow tract gradient >30 mm Hg caused a significant decrease of MBF. hMBF was adjusted simultaneously for resting MBF instead of using a ratio of hyperemic blood flow divided by resting blood flow because the latter quantity has ill-defined statistical properties. Myocardial ischemia and the magnitude of hypertrophy were considered putative causes of fibrosis. Therefore, logistic regression model analysis was used to analyze the incidence of myocardial fibrosis and to determine whether its likelihood is associated with end-diastolic wall thickness and hMBF. The logistic regression model analysis with repeated measurements of fibrosis in each patient was performed with a general linear model with logit link and with mixed effects using linearization about the best linear unbiased predictors.²³ The Student *t* test for unpaired data was used for comparison of baseline characteristics for continuous variables, and the χ^2 test was used for categorical data (gender). Statistical significance was taken throughout at the 5% level ($P < 0.05$).

The authors had full access to and take full responsibility for the integrity of the data. All authors have read and agree to the manuscript as written.

Results

Study Population

Healthy controls and HCM patients differed only in LV mass index but not in age, gender, and other characteristics listed in Table 1. Overall, the HCM patient cohort was considered low risk according to clinical risk stratification and was mainly asymptomatic, with 68% in New York Heart Association class I (Table 2).³ In HCM patients, 475 of 560 segments (35×16 segments) were used for statistical analysis, with complete data in each of these segments for wall thickness, resting and stress perfusion, and delayed contrast enhancement. Incomplete data sets were mainly a result of gaps in

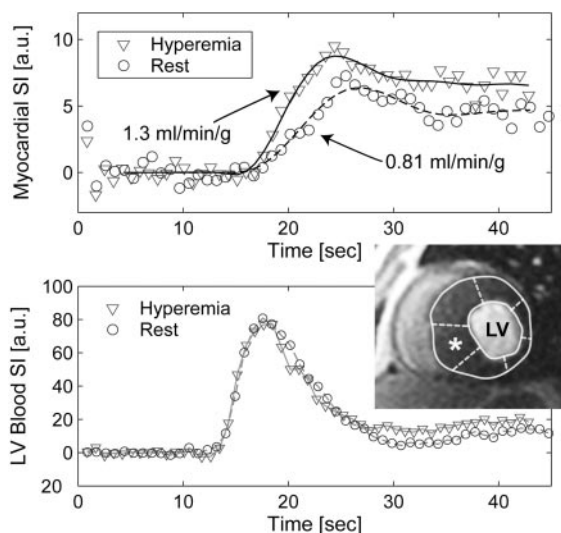


Figure 2. Quantitative myocardial perfusion at rest and during adenosine vasodilation in the same patient as in Figure 1. Top panel demonstrates the signal intensity (SI) curves (in arbitrary units [a.u.]) during the first pass of a contrast agent bolus in the hypertrophied basal myocardial segment (marked as *). Bottom panel represents the SI curves in the blood pool used as the arterial input function.

TABLE 2. Clinical Risk Stratification and Medications in HCM Patients

	HCM Patients (n=35)
NYHA class I/II/ III, % (n)	68.6/25.7/5.7 (24/9/2)
No. of SCD risk factors present (0/1/2/3 risk factors), % (n)	60/29/9/3 (21/10/3/1)
Family history of SCD	31.4 (11/35)
Unexplained syncope	5.7 (2/35)
NSVT on Holter monitor	8.6 (3/35)
Abnormal exercise blood pressure response	6.9 (2/29)*
Maximum LV wall thickness \geq 30 mm	2.9 (1/35)
Echocardiographic LV outflow tract gradient \geq 30 mm Hg	14.3 (5/35)
β -Blockers	42.9 (15/35)
Verapamil/diltiazem	5.7 (2/35)
Disopyramide	11.4 (4/35)
Amiodarone	17.1 (6/35)

Values are % (n/N) unless otherwise indicated. NYHA indicates New York Heart Association; SCD, sudden cardiac death; and NSVT, nonsustained ventricular tachycardia. For the number of risk factors present, family history of SCD, unexplained syncope, nonsustained ventricular tachycardia, abnormal blood pressure response during exercise, and maximum wall thickness \geq 30 mm were considered.

*Blood pressure response during exercise is not considered a valid risk factor in HCM patients >40 years of age.

perfusion data either because of insufficient data quality or because of acquisition of only 2 slices during adenosine infusion in patients with heart rates not allowing acquisition of a third slice. The contrast-to-noise ratio for all perfusion studies averaged 23:1 \pm 11:1 and was significantly higher during hyperemia (28:1 \pm 12:1) than during rest (18:1 \pm 7:1; P <0.001 for paired t test).

In HCM patients, 142 of 475 myocardial segments (29.9%) had an end-diastolic wall thickness >12 mm (range for the 475 segments, 1 to 34.5 mm; mean \pm SD, 10.9 \pm 5.0 mm), and

72 of 475 myocardial segments (15.2%) showed delayed gadolinium contrast enhancement. The extent of delayed contrast enhancement in segments with any delayed contrast enhancement ranged from 10% to 100% (mean \pm SD, 58.8 \pm 27.4%). The incidence of fibrosis (P <0.001) was found to increase significantly across quartiles of end-diastolic wall thickness (Figure 3A). In the logistic regression model, with end-diastolic wall thickness treated as a continuous variable, the odds for presence of delayed contrast enhancement in HCM patients were 1.13:1 for each millimeter increase in end-diastolic wall thickness (P <0.001).

In healthy controls, the end-diastolic wall thickness ranged from 3.5 to 11.9 mm (mean \pm SD, 7.3 \pm 1.8 mm).

A proportion of the 35 patients with HCM were on medications with potential confounding effects on MBF (Table 2): 15 took β -blockers (43%), 2 were treated with calcium channel inhibitors of the verapamil/diltiazem type (6%), 4 were treated with disopyramide (12%), and 6 were on amiodarone (17%).

Five of 35 HCM patients (14.3%) had a resting LV outflow tract gradient >30 mm Hg on echocardiography. This parameter was documented as a dichotomous variable because of intraindividual variability of this parameter and on the basis of the proposed cutoff of 30 mm Hg in a prospective study demonstrating its prognostic value.⁴

Myocardial Perfusion Reserve

Resting MBF averaged 0.71 \pm 0.27 mL/min per gram in HCM patients and 0.85 \pm 0.30 mL/min per gram in controls. Resting MBF, adjusted for age (P =0.58), gender (P <0.001), and resting rate pressure product (P <0.001), was similar in HCM patients and controls but with a significant (P <0.001) difference of 0.21 \pm 0.06 mL/min per gram between female and male subjects.

Myocardial fibrosis was observed more frequently in a segment with poor hyperemic response. Figure 3B demonstrates the decreasing incidence of fibrosis with increasing

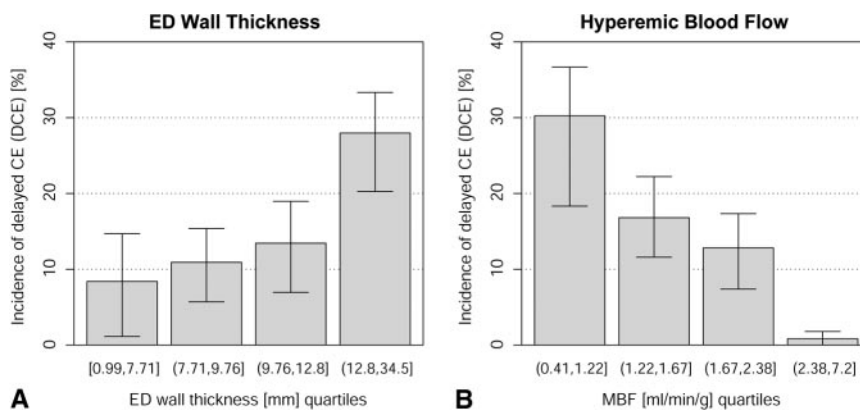


Figure 3. A, Within the HCM patients, the incidence of delayed contrast enhancement (CE) (DCE) within a segment increased with increasing end-diastolic (ED) wall thickness quartiles (odds ratio, 1.13:1 for each millimeter increase; P <0.001 for wall thickness as continuous variable in logistic regression model). Square brackets indicate inclusion, and round brackets indicate exclusion of a given end-diastolic wall thickness cut-point value in the respective quartile range. Error bars represent the 95% CIs for incidence of delayed contrast enhancement and were obtained by bootstrap with sampling by subject. B, The incidence of fibrosis in a myocardial segment decreased with increasing hyperemic blood flow, with incidence shown by quartile of hMBF. With hyperemic blood flow treated as a continuous variable in a logistic regression model, the odds for fibrosis decreased by 2.2:1 (P <0.01) for each 1 mL/min per gram increase of hyperemic blood flow (P <0.01), with simultaneous adjustment by age and gender.

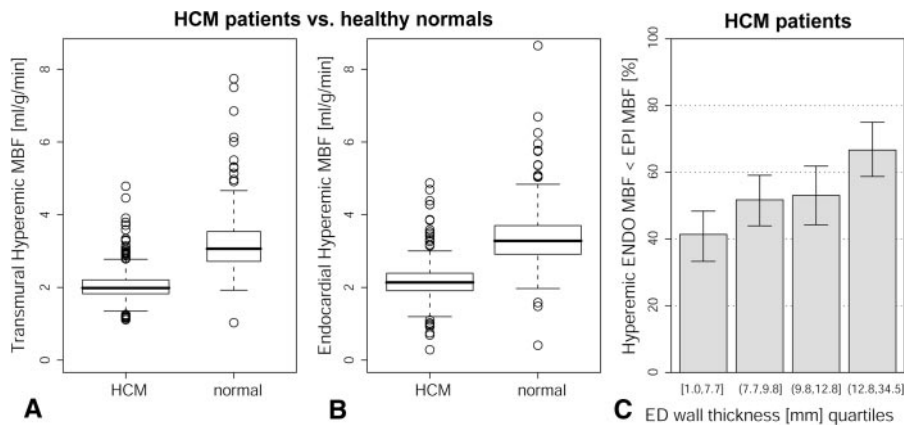


Figure 4. A, HCM patients have significantly ($P<0.001$) lower hMBF than healthy controls after adjustment for differences in age, gender distribution, wall thickness, rest perfusion, and extent of delayed contrast enhancement. B, Similar to the transmural average of hMBF in each myocardial sector, endocardial hMBF, after adjustment for age, gender, and resting MBF ($P<0.01$), was lower in HCM patients than in healthy controls, and endocardial hMBF was significantly higher than the epicardial hMBF in normal subjects ($P<0.05$) but not in HCM patients. C, Within the HCM patients, the incidence of hMBF in the endocardial layer (ENDO) was less than hMBF in the epicardial layer (EPI) and increased over quartiles of end-diastolic (ED) wall thickness ($P=0.03$), suggesting that an adverse reduction of hMBF occurs preferentially in the endocardial layer. Square brackets indicate inclusion, and round brackets indicate exclusion of a given end-diastolic wall thickness cut-point value in the respective quartile range. Error bars represent the 95% CIs.

hyperemic blood flow. The odds for fibrosis in a myocardial segment increased by 2.2:1 ($P<0.01$) for each 1 mL/min per gram decrease of hyperemic blood flow ($P<0.01$), with simultaneous adjustment for age ($P=0.11$) and gender ($P=0.11$).

The average of hMBF in HCM patients was 1.84 ± 0.89 mL/min per gram in HCM patients and lower than the mean of 3.42 ± 1.76 mL/min per gram in healthy controls ($P<0.01$ for t test of per-subject means of MBF between HCM patients and healthy controls). hMBF in myocardial segments remained significantly lower in HCM patients (by -0.95 ± 0.30 [SE] mL/min per gram; $P<0.001$), with adjustment for age ($P=0.13$), gender ($P=0.90$), end-diastolic segmental wall thickness (-0.013 ± 0.004 [SE] mL/min per gram per millimeter wall thickness; $P<0.001$), resting MBF ($P<0.001$), presence of LV outflow tract gradient >30 mm Hg ($P=0.06$), and extent of delayed contrast enhancement ($P=0.95$) in the linear mixed-effects model (Figure 4A). hMBF in the endocardial layer of myocardial segments was lower by -1.23 ± 0.39 mL/min per gram in HCM patients than in normal volunteers ($P=0.001$), with simultaneous adjustment for age, gender, end-diastolic wall thickness ($P<0.001$), resting MBF ($P<0.001$), presence of LV outflow tract gradient >30 mm Hg, and extent of delayed contrast enhancement ($P=0.64$). The ratio of endocardial to epicardial hMBF averaged over all segments was 1.08:1 in healthy controls and 0.99:1 in HCM patients ($P=0.07$ for Wilcoxon rank sum test). Within the HCM patients, the incidence of a hyperemic endocardial hMBF lower than epicardial hMBF increased over quartiles of end-diastolic wall thickness ($P=0.03$; odds increased by 1.05:1 per millimeter increase of end-diastolic wall thickness), suggesting a preferential reduction of hMBF in the endocardial layer with increasing magnitude of hypertrophy (Figure 4C).

Within the group of HCM patients, hMBF decreased by 0.011 mL/min per gram (SE 0.0035) for each millimeter increase of end-diastolic wall thickness ($P<0.005$), with

simultaneous adjustment for age ($P=0.27$), gender difference ($P=0.74$), resting MBF ($P<0.001$), extent of contrast hyper-enhancement (ie, fibrosis) ($P=0.48$), and presence of LV outflow tract gradient of >30 mm Hg (coefficient mean \pm SE, -0.86 ± 0.33 mL/min per gram; $P<0.02$). Similarly, in the endocardial layer, hMBF decreased by 0.017 mL/min per gram (SE 0.003) for each millimeter increase of end-diastolic wall thickness. Figure 5 shows the transmural and endocardial layer averages of hMBF by quartiles of end-diastolic wall thickness. hMBF in the endocardial layer was modeled as a function of the transmural hMBF or epicardial hMBF and end-diastolic wall thickness (quartile) categories. The rate at which endocardial hMBF increases with transmural or epicardial hMBF was reduced significantly for the 2 highest end-diastolic wall thickness quartiles ($P<0.05$), with the most pronounced interaction effect in the highest end-diastolic wall thickness quartile.

Discussion

In the present MRI study, we demonstrate in patients with HCM a reduced myocardial perfusion reserve as measured by hMBF, particularly in the endocardium, and in proportion to the magnitude of hypertrophy. It has been shown that the magnitude of hypertrophy is related directly to the risk of sudden death,²⁴ but the pathophysiological mechanisms of sudden death remain largely unknown. It was observed previously that the vasodilator response is impaired in HCM in both hypertrophied and nonhypertrophied wall segments.¹⁰ The association of vasodilator response impairment and end-diastolic wall thickness observed in the present study indicates that ischemia is more prevalent and more severe in hypertrophied segments. The diagnosis of HCM was in itself associated with a significant reduction of hMBF with simultaneous multivariable adjustment, including end-diastolic wall thickness, LV outflow tract gradient >30 mm Hg, and extent of delayed contrast enhancement. This suggests that the vasodilator response in HCM patients is already impaired

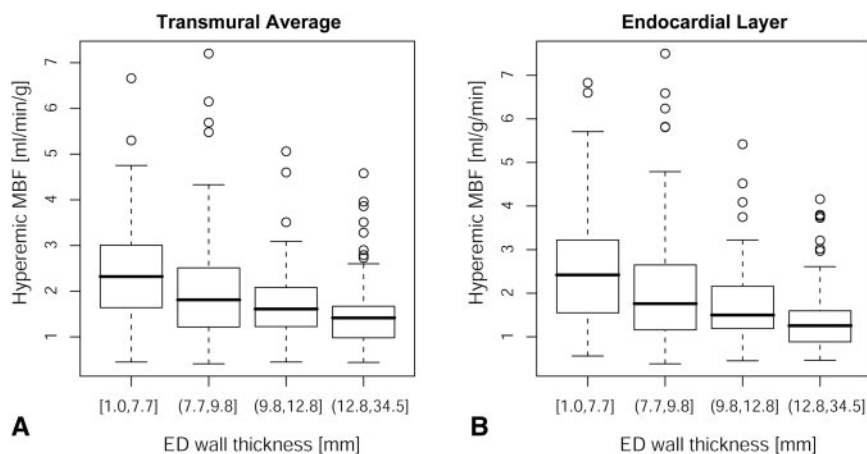


Figure 5. A, Transmural hMBF declined significantly with end-diastolic (ED) wall thickness in HCM patients and averaged 0.011 mL/min per gram (SE 0.0035) for each millimeter increase of ED wall thickness ($P < 0.005$), with simultaneous adjustment for age, gender, resting MBF, extent of contrast hyperenhancement (ie, fibrosis), and presence of LV outflow tract gradient of >30 mm Hg (-0.86 ± 0.33 mL/min per gram; $P < 0.02$). B, In the endocardial layer, the hMBF showed an average 0.017 mL/min per gram (SE 0.003) decline for each millimeter increase of end-diastolic wall thickness ($P < 0.005$), and this rate of decline was significantly higher in comparison to the epicardial layer ($P < 0.002$ for interaction of myocardial layer with wall thickness).

in segments without hypertrophy and decreases further with hypertrophy. Furthermore, our finding of decreased incidence of myocardial fibrosis with increasing hMBF may suggest a pathophysiological link between repetitive hypoperfusion during stress and development of myocardial fibrosis. The unique ability of cardiac MRI to match perfusion and myocardial fibrosis data in a single investigation thus provides novel insights into a potential mechanism for the development of myocardial fibrosis in HCM patients. It is tempting to speculate that hypoperfusion and/or the associated fibrosis may contribute to the increased risk of sudden cardiac death during or after strenuous physical exercise in these patients.

Myocardial perfusion and perfusion reserve have been shown to be of prognostic value in patients with HCM, and these parameters may become an integral part of clinical risk stratification.⁵ Elliott and colleagues³ introduced the concept of risk factor burden, including syncope and family history of sudden cardiac death, nonsustained ventricular tachycardia, abnormal blood pressure response, and marked LV hypertrophy (>30 mm). The use of MRI in the present study provided the important advantage of spatially matched, high-resolution measurements of LV hypertrophy, MBF, and myocardial fibrosis all made within 1 MRI study of <60 minutes in duration.^{25–27} We found reduced hMBF in HCM patients with and without hypertrophy. This is consistent with PET data demonstrating impaired microvascular function in both hypertrophied and nonhypertrophied myocardium in such patients,¹⁰ although the resolution of PET is suboptimal for assessing the magnitude of hypertrophy. In addition, myocardial fibrosis, a possibly important confounding factor, could also be assessed directly in the present MRI study with high spatial resolution. Although the results are reported here for a standardized American Heart Association segment model, the underlying measurements are made with resolution sufficient to investigate perfusion, viability, and function in the endocardial and epicardial layers and to show a higher predisposition of the endocardial layer to ischemia. An MRI study previously showed, in a selected cohort of patients with the Asp175Asn mutation of the α -tropomyosin gene, an association between perfusion and LV hypertrophy by a semiquantitative approach rather than by an absolute quantification of MBF.²⁸ Furthermore, myocardial fibrosis was not assessed in that previous MRI study, and a confounding of myocardial

fibrosis with perfusion impairments could not be excluded. The present study clearly demonstrates a higher incidence of myocardial fibrosis with increasing wall thickness, in agreement with work by other groups,^{29–31} but the inverse relationship of LV hypertrophy and perfusion reserve still remains after adjustment for the extent of fibrosis. The identified association between LV hypertrophy and hMBF exists in both patients with and patients without outflow tract obstruction, suggesting that perfusion reserve as a risk factor does not simply reflect obstruction, an emerging risk stratification parameter with prognostic importance.⁴ These findings suggest that LV hypertrophy should be interpreted as a continuous risk parameter rather than a dichotomous one with an arbitrary threshold. Furthermore, myocardial perfusion may hold additional prognostic information over LV wall thickness measurements as part of clinical risk stratification, which may be particularly valuable in patients with mild LV hypertrophy and few clinical risk factors, as demonstrated in our low-risk HCM cohort.

MBF quantification by first-pass MRI has been validated in experimental work with the use of microspheres.^{13,32,33} In the present study we used a smaller dosage of Gd-DTPA contrast than in most previous studies to maintain a linear relation between signal and contrast concentration, an important assumption of the analysis. The majority of our flow data in both healthy volunteers and HCM patients at rest and during hyperemia are in agreement with previous studies using first-pass MRI and other modalities, such as PET.^{5,10,27} Slight deviations may be explained by differences in baseline characteristics, such as age, gender distribution, and blood pressure, because all of these substantially influence MBF.³⁴ In agreement with data from Camici and colleagues,¹⁰ we confirmed that the MBF at rest in HCM was not different from that in healthy controls, and this finding was independent of wall thickness, myocardial fibrosis, and other potential confounders.

Recently, we demonstrated decreased MBF at rest in myocardial segments with significant amounts of delayed contrast enhancement in patients with ischemic heart disease.¹⁴ Similarly, in our HCM cohort we observed a significant association between hMBF and the extent of myocardial fibrosis as measured by delayed contrast enhancement.

We have demonstrated preferential reduction of endocardial hMBF with increasing wall thickness. With the use of the superior spatial resolution of MRI over PET, this now allows new insights into the transmural blood flow distribution. A PET study has shown improved endocardial to epicardial blood flow ratios in hypertrophied septal segments after verapamil treatment of HCM patients despite unchanged total MBF. Endocardial and epicardial flows could not be assessed in nonhypertrophied segments because of the spatial resolution limit of PET in that study of ≈ 6 mm.¹¹ Muehling and colleagues³⁵ have demonstrated the feasibility of establishing a normal range of distribution of endocardial and epicardial MBF at rest and during administration of adenosine in myocardium of young healthy volunteers with normal wall thickness using first-pass MRI.

There may have been some selection bias in the present study. HCM patients with a high risk of sudden cardiac death and an internal cardioverter-defibrillator device were excluded from this study (MRI contraindication), as well as patients with higher-degree atrioventricular block (adenosine contraindication). Our patient cohort is thus predominantly at low risk of sudden cardiac death. This may be viewed as a strength of the study, suggesting a potential role for hMBF in the risk assessment of relatively lower-risk patients.

In conclusion, our present study shows that in HCM perfusion reserve is reduced, particularly in the endocardium, and in proportion to the magnitude of hypertrophy. Thus, microvascular dysfunction and ischemia may be important components of the risk attributable to hypertrophy in HCM, and future clinical risk assessment should include these parameters.

Sources of Funding

This study was supported by grants from the German Academic Exchange Service (to Dr Petersen), the British Heart Foundation (to Dr Petersen, L. Hudsmith, Dr Selvanayagam, Dr Neubauer, and Dr Watkins) and the Wellcome Trust (to Drs Neubauer and Watkins). Dr Jerosch-Herold was supported by R01 HL65394 from the National Institutes of Health. Dr Neubauer received research support from Siemens Medical Solutions.

Disclosures

None.

References

- Spirito P, Seidman CE, McKenna WJ, Maron BJ. The management of hypertrophic cardiomyopathy. *N Engl J Med*. 1997;336:775–785.
- Maron BJ, Shirani J, Poliac LC, Mathenge R, Roberts WC, Mueller FO. Sudden death in young competitive athletes: clinical, demographic, and pathological profiles. *JAMA*. 1996;276:199–204.
- Elliott PM, Poloniecki J, Dickie S, Sharma S, Monserrat L, Varnava A, Mahon NG, McKenna WJ. Sudden death in hypertrophic cardiomyopathy: identification of high risk patients. *J Am Coll Cardiol*. 2000;36:2212–2218.
- Maron MS, Olivetto I, Betocchi S, Casey SA, Lesser JR, Losi MA, Cecchi F, Maron BJ. Effect of left ventricular outflow tract obstruction on clinical outcome in hypertrophic cardiomyopathy. *N Engl J Med*. 2003;348:295–303.
- Cecchi F, Olivetto I, Gistri R, Lorenzoni R, Chiriatti G, Camici PG. Coronary microvascular dysfunction and prognosis in hypertrophic cardiomyopathy. *N Engl J Med*. 2003;349:1027–1035.
- Moon JC, McKenna WJ, McCrohon JA, Elliott PM, Smith GC, Pennell DJ. Toward clinical risk assessment in hypertrophic cardiomyopathy with

- gadolinium cardiovascular magnetic resonance. *J Am Coll Cardiol*. 2003;41:1561–1567.
- Olivetto I, Cecchi F, Gistri R, Lorenzoni R, Chiriatti G, Girolami F, Torricelli F, Camici PG. Relevance of coronary microvascular flow impairment to long-term remodeling and systolic dysfunction in hypertrophic cardiomyopathy. *J Am Coll Cardiol*. 2006;47:1043–1048.
- Dilsizian V, Bonow RO, Epstein SE, Fananapazir L. Myocardial ischemia detected by thallium scintigraphy is frequently related to cardiac arrest and syncope in young patients with hypertrophic cardiomyopathy. *J Am Coll Cardiol*. 1993;22:796–804.
- Lorenzoni R, Gistri R, Cecchi F, Olivetto I, Chiriatti G, Elliott P, McKenna WJ, Camici PG. Coronary vasodilator reserve is impaired in patients with hypertrophic cardiomyopathy and left ventricular dysfunction. *Am Heart J*. 1998;136:972–981.
- Camici P, Chiriatti G, Lorenzoni R, Bellina RC, Gistri R, Italiani G, Parodi O, Salvadori PA, Nista N, Papi L, L'Abbate A. Coronary vasodilation is impaired in both hypertrophied and nonhypertrophied myocardium of patients with hypertrophic cardiomyopathy: a study with nitrogen-13 ammonia and positron emission tomography. *J Am Coll Cardiol*. 1991;17:879–886.
- Choudhury L, Elliott P, Rimoldi O, Ryan M, Lammertsma AA, Boyd H, McKenna WJ, Camici PG. Transmural myocardial blood flow distribution in hypertrophic cardiomyopathy and effect of treatment. *Basic Res Cardiol*. 1999;94:49–59.
- Maron BJ, Wolfson JK, Epstein SE, Roberts WC. Intramural ("small vessel") coronary artery disease in hypertrophic cardiomyopathy. *J Am Coll Cardiol*. 1986;8:545–557.
- Jerosch-Herold M, Swingen C, Seethamraju RT. Myocardial blood flow quantification with MRI by model-independent deconvolution. *Med Phys*. 2002;29:886–897.
- Selvanayagam JB, Jerosch-Herold M, Porto I, Sheridan D, Cheng AS, Petersen SE, Searle N, Channon KM, Banning AP, Neubauer S. Resting myocardial blood flow is impaired in hibernating myocardium: a magnetic resonance study of quantitative perfusion assessment. *Circulation*. 2005;112:3289–3296.
- Richardson P, McKenna W, Bristow M, Maisch B, Mautner B, O'Connell J, Olsen E, Thiene G, Goodwin J, Gyrfas I, Martin I, Nordet P. Report of the 1995 World Health Organization/International Society and Federation of Cardiology Task Force on the Definition and Classification of cardiomyopathies. *Circulation*. 1996;93:841–842.
- Petersen SE, Jung BA, Wiesmann F, Selvanayagam JB, Francis JM, Hennig J, Neubauer S, Robson MD. Myocardial tissue phase mapping with cine phase-contrast MR imaging: regional wall motion analysis in healthy volunteers. *Radiology*. 2006;238:816–826.
- Corqueira MD, Weissman NJ, Dilsizian V, Jacobs AK, Kaul S, Laskey WK, Pennell DJ, Rumberger JA, Ryan T, Verani MS. Standardized myocardial segmentation and nomenclature for tomographic imaging of the heart: a statement for healthcare professionals from the Cardiac Imaging Committee of the Council on Clinical Cardiology of the American Heart Association. *Circulation*. 2002;105:539–542.
- Simonetti OP, Kim RJ, Fieno DS, Hillenbrand HB, Wu E, Bundy JM, Finn JP, Judd RM. An improved MR imaging technique for the visualization of myocardial infarction. *Radiology*. 2001;218:215–223.
- Selvanayagam JB, Petersen SE, Francis JM, Robson MD, Kardos A, Neubauer S, Taggart DP. Effects of off-pump versus on-pump coronary surgery on reversible and irreversible myocardial injury: a randomized trial using cardiovascular magnetic resonance imaging and biochemical markers. *Circulation*. 2004;109:345–350.
- Jerosch-Herold M, Hu X, Murthy NS, Seethamraju RT. Time delay for arrival of MR contrast agent in collateral-dependent myocardium. *IEEE Trans Med Imaging*. 2004;23:881–890.
- Selvanayagam JB, Porto I, Channon K, Petersen SE, Francis JM, Neubauer S, Banning AP. Troponin elevation after percutaneous coronary intervention directly represents the extent of irreversible myocardial injury: insights from cardiovascular magnetic resonance imaging. *Circulation*. 2005;111:1027–1032.
- Pinheiro JC, Bates DM. *Mixed-Effects Models in S and S-Plus*. New York, NY: Springer-Verlag; 2000.
- Venables WN, Ripley BD. *Modern Applied Statistics With S*. 4th ed. New York, NY: Springer-Verlag; 2002.
- Spirito P, Bellone P, Harris KM, Bernabo P, Bruzzi P, Maron BJ. Magnitude of left ventricular hypertrophy and risk of sudden death in hypertrophic cardiomyopathy. *N Engl J Med*. 2000;342:1778–1785.
- Hudsmith LE, Petersen SE, Francis JM, Robson MD, Neubauer S. Normal human left and right ventricular and left atrial dimensions using

- steady state free precession magnetic resonance imaging. *J Cardiovasc Magn Reson*. 2005;7:775–782.
26. Mahrholdt H, Wagner A, Holly TA, Elliott MD, Bonow RO, Kim RJ, Judd RM. Reproducibility of chronic infarct size measurement by contrast-enhanced magnetic resonance imaging. *Circulation*. 2002;106:2322–2327.
 27. Muhling OM, Dickson ME, Zenovich A, Huang Y, Wilson BV, Wilson RF, Anand IS, Seethamraju RT, Jerosch-Herold M, Wilke NM. Quantitative magnetic resonance first-pass perfusion analysis: inter- and intraobserver agreement. *J Cardiovasc Magn Reson*. 2001;3:247–256.
 28. Sipola P, Lauerma K, Husso-Saastamoinen M, Kuikka JT, Vanninen E, Laitinen T, Manninen H, Niemi P, Peuhkurinen K, Jaaskelainen P, Laakso M, Kuusisto J, Aronen HJ. First-pass MR imaging in the assessment of perfusion impairment in patients with hypertrophic cardiomyopathy and the Asp175Asn mutation of the alpha-tropomyosin gene. *Radiology*. 2003;226:129–137.
 29. Matsunaka T, Hamada M, Matsumoto Y, Higaki J. First-pass myocardial perfusion defect and delayed contrast enhancement in hypertrophic cardiomyopathy assessed with MRI. *Magn Reson Med Sci*. 2003;2:61–69.
 30. Moon JC, Mogensen J, Elliott PM, Smith GC, Elkington AG, Prasad SK, Pennell DJ, McKenna WJ. Myocardial late gadolinium enhancement cardiovascular magnetic resonance in hypertrophic cardiomyopathy caused by mutations in troponin I. *Heart*. 2005;91:1036–1040.
 31. Soler R, Rodriguez E, Monserrat L, Mendez C, Martinez C. Magnetic resonance imaging of delayed enhancement in hypertrophic cardiomyopathy: relationship with left ventricular perfusion and contractile function. *J Comput Assist Tomogr*. 2006;30:412–420.
 32. Hsu LY, Rhoads KL, Holly JE, Kellman P, Aletas AH, Arai AE. Quantitative myocardial perfusion analysis with a dual-bolus contrast-enhanced first-pass MRI technique in humans. *J Magn Reson Imaging*. 2006;23:315–322.
 33. Christian TF, Rettmann DW, Aletas AH, Liao SL, Taylor JL, Balaban RS, Arai AE. Absolute myocardial perfusion in canines measured by using dual-bolus first-pass MR imaging. *Radiology*. 2004;232:677–684.
 34. Wang L, Jerosch-Herold M, Jacobs DR Jr, Shahar E, Folsom AR. Coronary risk factors and myocardial perfusion in asymptomatic adults: the Multi-Ethnic Study of Atherosclerosis (MESA). *J Am Coll Cardiol*. 2006;47:565–572.
 35. Muehling OM, Jerosch-Herold M, Panse P, Zenovich A, Wilson BV, Wilson RF, Wilke N. Regional heterogeneity of myocardial perfusion in healthy human myocardium: assessment with magnetic resonance perfusion imaging. *J Cardiovasc Magn Reson*. 2004;6:499–507.

CLINICAL PERSPECTIVE

In the younger population, particularly in athletes, hypertrophic cardiomyopathy (HCM) remains among the most common causes for sudden cardiac death. Cardiac microvascular dysfunction in HCM may create an ischemic substrate potentially contributing to a milieu promoting arrhythmia. It remains unknown whether extent of hypertrophy is associated with proportionally poorer perfusion reserve. Cardiac magnetic resonance imaging was performed to study the interrelations between end-diastolic wall thickness, resting and hyperemic myocardial blood flow, and extent of myocardial fibrosis. Although myocardial blood flow was preserved at rest in HCM patients, during adenosine-induced hyperemia the blood flow reserve was reduced in comparison to healthy controls, and the magnitude of blunted flow reserve was related to the degree of hypertrophy and particularly in the endocardial layer. The incidence of myocardial fibrosis increased with increasing end-diastolic wall thickness. These findings suggest that in HCM the vasodilator reserve is reduced, particularly in the endocardium, and in proportion to the magnitude of hypertrophy. Microvascular dysfunction, subsequent ischemia, and myocardial fibrosis may be important contributors to natural history in HCM.

On-line addendum to “Evidence For Microvascular Dysfunction In Hypertrophic Cardiomyopathy – New Insights From Multi-Parametric Magnetic Resonance Imaging”

Steffen E. Petersen¹, Michael Jerosch-Herold², Lucy E. Hudsmith¹, Matthew D. Robson¹, Jane M. Francis¹, Helen A. Doll³, Joseph B. Selvanayagam¹, Stefan Neubauer¹, Hugh Watkins¹

From the ¹Department of Cardiovascular Medicine and OCMR, University of Oxford, UK, the ²Advanced Imaging Research Center, Oregon Health & Science University, OR, US and the ³Department of Public Health, University of Oxford, UK

Determination of Myocardial Blood Flow by Model-Independent Deconvolution

Signal intensity (SI) averages were measured for 16 myocardial sectors for each image of a dynamic series covering the first pass and recirculation of the injected contrast agent, using the AHA segmentation model. The resulting signal intensity curves and the associated times at which each image was acquired are used for determination of regional blood flow. Figure 1, reproduced here from the main body of the manuscript, provides an example of signal intensity changes in the inferior-septal segment, for rest and hyperemia. A region of interest (ROI) in the center of the left ventricle was used to sample signal intensity changes for the arterial input of contrast.

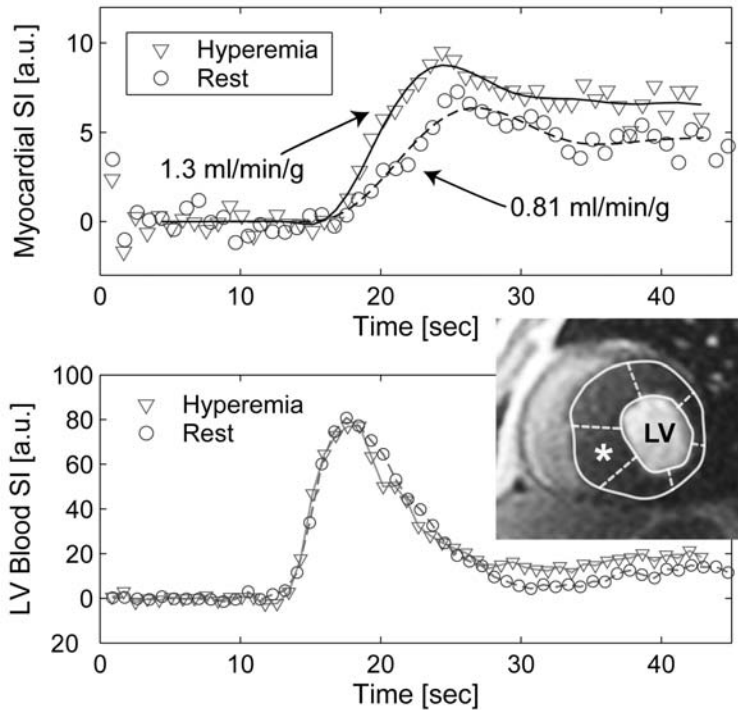


Figure 1 (reproduced from main body of manuscript): Quantitative myocardial perfusion at rest and during adenosine vasodilatation in the same patient as in figure 1. Top figure demonstrates the signal intensity (SI) curves (arbitrary units = a.u.) during the first pass of a contrast agent bolus in the hypertrophied basal myocardial segment (marked as *) and the bottom figure represents the SI curves in the blood pool used as the arterial input function.

The assumption of a linear relationship between signal intensity changes, and contrast agent concentration changes, is central for the analysis and estimation of blood flow from signal intensity curves. For this reason a T1-weighted sequence is used, with short echo-times to minimize the sensitivity to magnetic susceptibility and motion. Signal saturation is most likely to be observed in the left ventricular blood pool, because the contrast bolus is more compact in the LV blood pool than during transit through a tissue region of interest. With a contrast dosage of 0.25 mmol/kg, we estimate peak contrast concentrations in the LV blood pool to be on the order of 1.8 mmol/L with normal LV function.¹ For Gadodiamide, a concentration of 1.8 mmol/L corresponds to a peak relaxation rate constant of approximately 7 s^{-1} . Furthermore, it is important to minimize the effects of blood inflow in the ventricular cavity, i.e. the signal enhancement through inflow should be reduced by using a slice imaged during diastole to determine the arterial input function. Figure 2 shows the relation between signal and relaxation rate measured

in phantoms with a saturation recovery prepared gradient echo sequence as used in this study, and also illustrates how inflow could alter this relationship.

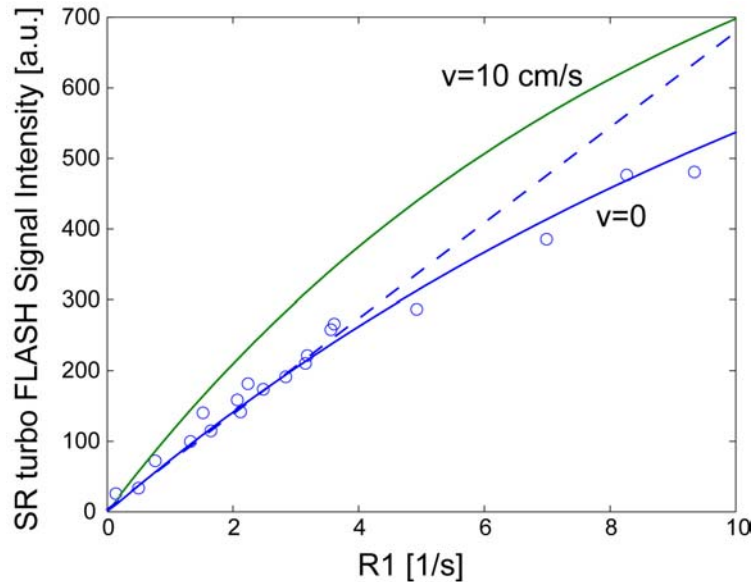


Figure 2: The circles show the relation between signal intensity, measured with a saturation-recovery prepared turbo FLASH sequence, and the relaxation rate in saline-filled phantoms doped with Gd-DTPA contrast agent. The R1 relaxation rate constant of the phantoms was determined with a spin-echo sequence. The evolution of the longitudinal magnetization of flowing blood, imaged with a non-slice-selective saturation recovery prepared turbo FLASH acquisition, was simulated using the approach of Peeters et al,² and assuming a linear phase encoding order. The blue solid line shows the simulation result for stationary fluid, while for the green curve a velocity of $v=10$ cm/s was assumed with otherwise identical parameters. The slice thickness was equal to 8 mm in the simulations. The dotted line represents a linear extrapolation from the region of low R1 values, and corresponds to the assumption of strict linear proportionality between signal intensity and signal, which was used for the analysis of the perfusion studies.

The central volume principle states that the tracer residue in a tissue region can be thought of as resulting from the convolution of the measured arterial input with the tissue residue impulse response. The tissue impulse response represents the tracer residue curve one would observe for a hypothetical arterial input equivalent to a very brief impulse. The tissue impulse response has some useful properties for blood flow estimation: The area under the tissue impulse response curve equals the effective distribution volume during the first pass, and the amplitude or height of the impulse response equals the blood flow in and out of the tissue ROI.^{3,4} The tissue impulse response, $R(t)$, cannot be measured directly, and the measured tissue residue curve, $q(t)$, equals the convolution integral for the arterial input function, $i(t)$, and the tissue impulse response, $R(t)$:⁴

$$q(t) = \int_0^t i(\tau) \cdot R(t - \tau) \cdot d\tau \quad (1)$$

To solution of this relationship for the tissue impulse response, $R(t)$, is equivalent to the process of differentiation, and division, both of which are much more sensitive to noise in the data, than integration. The numerical solution therefore needs to be stabilized by imposing some side constraints.

The process for calculating the impulse response was described previously, and summarized here briefly, with examples from the present study. The integral in equation [1] can be approximated by a sum over discrete time points $t=[t_1...t_n]$, that we assume equally spaced, with the sampling interval, Δt , defining the temporal resolution.⁵⁻⁷ The myocardial impulse response was represented as sum of B-splines, a generalization of the Bézier curve, which imposes some degree of smoothness:

$$R(t_i) = \sum_{j=1}^p B_j^{(k)}(t_i) \cdot \alpha_j \quad (2)$$

In the above sum $B_j^{(k)}$, represents a B-spline of order k , for the knot sequence $\tau_1 \leq \tau_2 \dots \leq \tau_{p+k}$, where $p+k$ is the number of knots⁸, and the α_j are weighting factors for the spline components. The problem of determining all $R(t_i)$ values of the impulse response is reduced to the determining the amplitudes, α_j , of the p spline components. The number of spline components (p) was set to 12, based on previous simulations, and $p \ll n$, where n is the number of time points in $R(t_i)$.

Regularization was used to assure that solving for the α_j coefficients does not suffer from numerical instability.^{5, 7} Regularization means that side-constraints are applied so that the addition of small amounts of noise to the measured data, would only result in relatively small changes in the impulse response, as one would expect for linear, “well-behaved” system. The weight given to the side constraint has to be chosen to balance the discrepancy between measured data and the calculated tissue residue curve, against the requirement of a reasonably smooth shape of the impulse response. A first order difference operator (L), applied to the B-spline coefficients, can be used for this purpose as a side constraint to reduce oscillations in the amplitudes of the B-spline coefficients. An L-shaped curve is obtained by plotting on a log-log scale the smoothness measure,

along the ordinate axis, versus the goodness of fit measure, along the abscissa, for different weightings of the smoothness side constraint.⁹ The horizontal part of the L-curve indicates the range of λ -values where the side-constraint causes the solution to be sufficiently smooth such that the value of the smoothness constraint changes little with the regularization parameter λ . The vertical part of the L-curve corresponds to solutions that give rise to small residuals, but the smoothness of the solution, varies dramatically with the regularization parameter. The optimal λ -value (λ_{opt}) corresponds to the location of the L-curve with the greatest curvature, i.e. the “corner” of the L-curve, i.e. before the impulse response starts to show large oscillations in amplitude if λ is further reduced.⁹⁻¹¹ The impulse response, $R(t)$, is calculated from equation 2 as a sum of B-splines with the coefficients (α_i) that are obtained with $\lambda=\lambda_{opt}$. Finally the predicted tissue response, is obtained through equation 1. Figure 3 shows the L curves that result from the tissue curves and the arterial inputs, corresponding to baseline and hyperemic states respectively, and shown in Figure 1.

The Gd-DTPA contrast agent can traverse the capillary barrier. As a result the impulse response shows an initial, relatively rapid decay, for the contrast that quickly transits through the capillary without escaping into the interstitial space. After this initial decay the impulse response falls off at a much slower rate that is not appreciable over the time period covered by the first pass measurements, partly reflux of contrast from the interstitial space into the vascular space only becomes detectable when the concentration of Gd-DTPA in the blood pool declines appreciably.

Other approaches, based on modeling of the transit and capillary exchange in the microcirculation have been used to estimate myocardial blood flow.^{12, 13} An advantage of the model-independent approach used in this study is the absence of model parameters, only a few of which can be optimized by fitting to the measured data, with others kept fixed at carefully chosen “default” settings. Therefore a largely model-independent approach has increasingly been used for analysis of myocardial perfusion with MRI.¹⁴⁻¹⁶

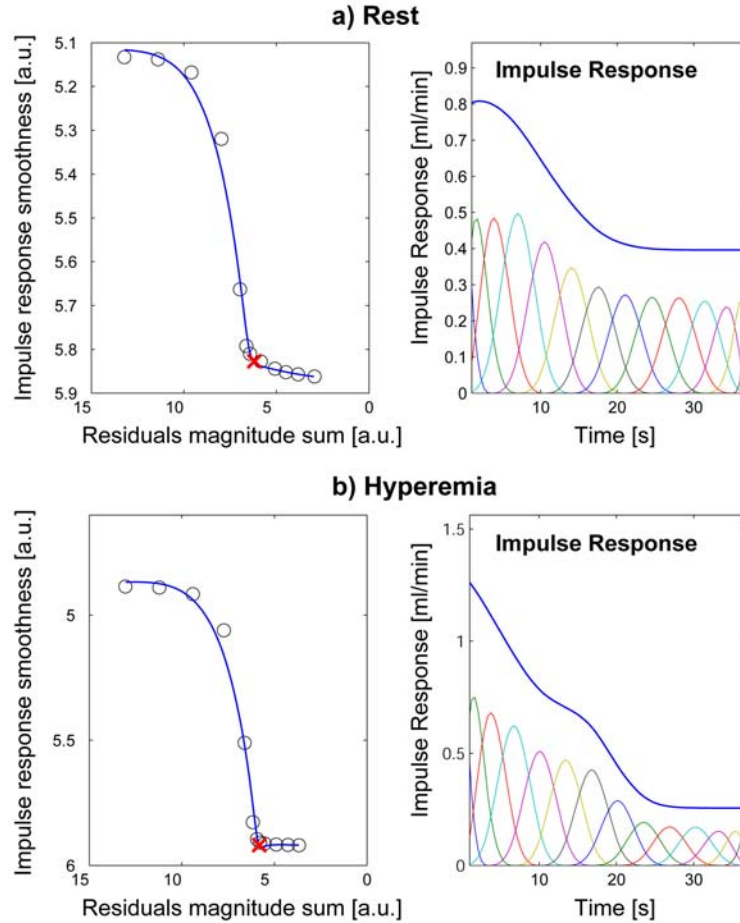


Figure 3: Left: The value of the smoothness side constraint for the impulse response is evaluated for a range of the regularization parameter λ and plotted against the sum of the residuals (magnitude) evaluated for the same values of λ , with the corresponding impulse response. The shape has an L-shaped knee and the corresponding value of λ represents an optimal choice for the regularization parameter. Right: The impulse response, shown here for rest (top) and hyperemia (bottom), was represented as a sum of B-splines. This B-spline representation was chosen to improve the numerical stability of the deconvolution process. The tissue impulse response curves shown here correspond to the optimal choices of the regularization parameter. The blood flow is estimated from the amplitude of the impulse response.

Cited Literature

1. Jerosch-Herold M, Wilke N, Stillman AE, Wilson RF. MR quantification of the myocardial perfusion reserve with a Fermi function model for constrained deconvolution. *Medical Physics*. 1998;25(1):73-84.
2. Peeters F, Annet L, Hermoye L, Van Beers BE. Inflow correction of hepatic perfusion measurements using T1-weighted, fast gradient-echo, contrast-enhanced MRI. *Magn Reson Med*. Apr 2004;51(4):710-717.
3. Zierler KL. Theoretical basis of indicator-dilution methods for measuring flow and volume. *Circulation Research*. 1962;10:393-407.
4. Zierler KL. Equations for measuring blood flow by external monitoring of radioisotopes. *Circulation Research*. 1965;16:309-321.
5. Jerosch-Herold M, Hu X, Murthy NS, Seethamraju RT. Time Delay for Arrival of MR Contrast Agent in Collateral-Dependent Myocardium. *IEEE Transactions on Medical Imaging*. 2004(in press).
6. Jerosch-Herold M, Seethamraju RT, Swingen CM, Wilke NM, Stillman AE. Analysis of myocardial perfusion MRI. *J Magn Reson Imaging*. Jun 2004;19(6):758-770.
7. Jerosch-Herold M, Swingen C, Seethamraju RT. Myocardial blood flow quantification with MRI by model-independent deconvolution. *Medical Physics*. 2002;29(5):886-897.
8. deBoor C. *A Practical Guide to Splines*. Vol 27. New York, NY: Springer Verlag; 1978.
9. Hansen PC. *Rank-deficient and discrete ill-posed problems*. Philadelphia: Society for Industrial and Applied Mathematics; 1998.
10. Hansen PC. Analysis of discrete ill-posed problems by means of the L-curve. *SIAM Review*. 1992;34(4):561-580.
11. Johnston PR, Gulrajani RM. Selecting the corner in the L-curve approach to Tikhonov regularization. *IEEE Trans. Biomed. Eng.* 2000;47(9):1293.
12. Schmitt M, Viallon M, Thelen M, Schreiber WG. Quantification of myocardial blood flow and blood flow reserve in the presence of arterial dispersion: a simulation study. *Magn Reson Med*. 2002;47(4):787-793.
13. Kroll K, Wilke N, Jerosch-Herold M, Wang Y, Zhang Y, Bache RJ, Basingthwaighte JB. Accuracy of modeling of regional myocardial flows from residue functions of an intravascular indicator. *Am J Physiol (Heart Circ Physiol)*. 1996;40:H1643-H1655.
14. Selvanayagam J, Jerosch-Herold M, Porto I, Sheridan D, Searle N, Doll H, Petersen S, Cheng A, Channon K, Banning A, Neubauer S. Resting myocardial blood flow is impaired in hibernating myocardium: an MR study of quantitative perfusion assessment. *Circulation*. 2005 (in press).

- 15.** Hsu LY, Rhoads KL, Holly JE, Kellman P, Aletras AH, Arai AE. Quantitative myocardial perfusion analysis with a dual-bolus contrast-enhanced first-pass MRI technique in humans. *J Magn Reson Imaging*. Mar 2006;23(3):315-322.
- 16.** Christian TF. The use of perfusion imaging in acute myocardial infarction: applications for clinical trials and clinical care. *Journal of Nuclear Cardiology*. 1995;2(5):423-436.